Journal of Statistical Physics, Vol. 101, Nos. 1/2, 2000

Reaction–Diffusion Patterns in Confined Chemical Systems

P. De Kepper,[1] E. Dulos,[1] J. Boissonade,[1] A. De Wit,[2] G. Dewel,[2] and P. Borckmans[2]

Received December 31, 1999

We review on the effects of the feed mode on pattern selection observed in chemical systems operated in open spatial reactors. In two-side-fed reactors, strong parameter ramps naturally confine patterns in a stratum. The reactor thickness acts both as a genuine bifurcation parameter and on the pattern dimensionality. Depending on that thickness, standard 2D hexagon and stripe Turing patterns or more complex 3D planforms are observed. In thin one-side-fed reactors, patterning process must escape the imposed fixed boundary conditions either by devices introducing mixed boundary conditions or by an intrinsic phenomenon dubbed "spatial bistability." We show that in most cases, for a comprehensive understanding of experimental observations, the full 3D aspects have to be taken into account.

KEY WORDS: Reaction–diffusion; chemical pattern; Turing structure; nonlinear dynamics; boundary conditions.

1. INTRODUCTION

The formation of nonequilibrium stationary reaction–diffusion patterns has been first predicted by Turing[1] in 1952. Their theoretical study has been boosted by the Brussels group, in particular by G. Nicolis who played a major role in the introduction of the bifurcation theory in the field.[2, 3] Nevertheless, their first experimental evidence occurred in 1990.[4]

[1] Centre de Recherche Paul Pascal, C.N.R.S. and Université Bordeaux I, Avenue Schweitzer, F-33600 Pessac, France.

[2] Service de Chimie-Physique and Center for Nonlinear Phenomena and Complex Systems, CP 231, Campus Plaine, Université Libre de Bruxelles, Blvd du Triomphe, B-1050 Bruxelles, Belgium.

0022-4715/00/1000-0495$18.00/0

Since their discovery, Turing structures have been extensively studied for nearly ten years. Most of the encountered experimental features can be explained in terms of selection between patterns of various symmetries,[5–8] or of patterns resulting from front interactions and instabilities.[9, 10] However, the quantitative analytical description of the actual experimental results still lags behind because of the presence of space dependent ramps of parameters. Indeed, to obtain the true asymptotic states, the reactors must be fed continuously. This is achieved by diffusing the chemical species from the boundaries in a gel-reactor in order to avoid perturbations through hydrodynamic flows. The resulting concentration profiles (ramps) orthogonal to the feed surfaces are usually strong and make it difficult, in general, to avoid three-dimensional aspects. Moreover, experiments seem to show that the presence of steep ramps favors the stacking of two-dimensional patterns[11] rather than genuine three-dimensional structures. Theory has, for the most part, considered ideally uniformly constrained systems in two and three spatial dimensions and the influence of weak ramps thereupon. Because the Turing and Hopf instabilities rely on the same kinetic mechanisms (competition between positive and negative feedbacks), Turing–Hopf interactions may also be studied[12–15] but will only be alluded to here.

In this paper, we will mainly draw the attention to the effects of the actual feeding of the reactor that generates concentration gradients and determines the boundary conditions in the problem. We will separately discuss this for the main two classes of reactors used until this day. These essentially differ by their feeding geometries: two-side-fed reactors with complementary subsets of chemicals or one-side-fed reactors with the full set of chemicals. We report on results obtained using the CIMA (chlorite, iodide, malonic acid) reaction and two other related reactions, the CDIMA (chlorine dioxide, iodine, malonic acid) and the CDI (chlorine dioxide, iodide reactions. The kinetic mechanisms of these reactions have been extensively analyzed by the group in Brandeis.[16]

In all these reactions, iodide and chlorite play a major role in respectively controlling the activatory and inhibitory kinetic processes at the origin of oscillations. Generally, patterns are made visible by introducing an "iodine color indicator" such as starch (amylose) or polyvinylalcohol. It is noteworthy that these color indicators also play an essential role in pattern formation since they enable the selective slowing down of the effective diffusivity of iodide, a species controlling the activatory kinetic path. This is a necessary condition for Turing and other spatial instabilities to develop. The slowing down is due to the formation of a reversible complex between the macromolecular color indicator, immobilized in the gel, and the iodine–iodide complex.[17, 18]

2. TWO-SIDE-FED REACTORS AND PARAMETER GRADIENTS

Based on an idea initially proposed by one of us,[19] Turing patterns were first obtained in open spatial reactors fed by diffusion from two opposing sides, with two different subsets of chemicals (Fig. 1a). This feed mode naturally induces cross ramps of chemical concentrations between the two feed surfaces and, as experimentally observed, pattern development is confined in a stratum of width Δ parallel to the feed boundaries where appropriate chemical parameter values are met. This is straightforward

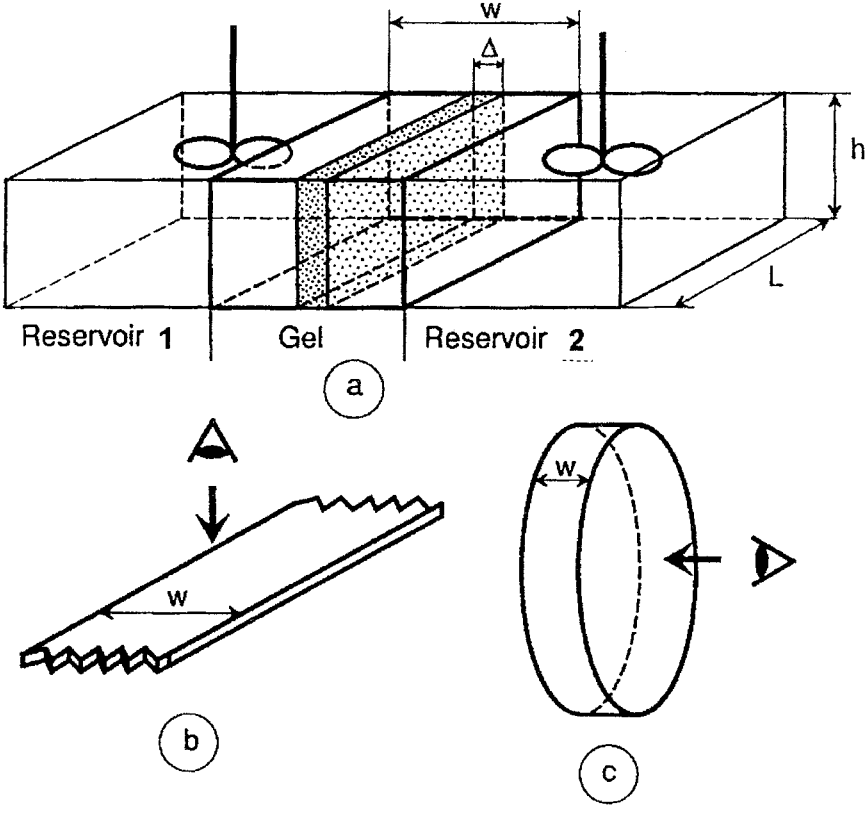

Fig. 1. Sketches of open spatial reactors. (a) Basic principles: The reactor proper consists of a block of hydrogel ($L \times h \times w$) in contact with the contents of two separated reservoirs (1 and 2). Reservoirs are vigorously stirred and continuously fed with fresh solutions of reagents. L and h are the geometric dimensions of the feed surfaces of the gel reactor and w is the width of the gel, the distance between the reservoirs. Δ is the width overwhich the chemical pattern, of characteristic wavelength λ, develops. (b) Thin strip reactor, $h \simeq \lambda \ll L$. Typical dimensions: $L = 20$ mm; $h = 0.2$ mm; $w = 3$ mm. (c) Disc reactor, $L = h \gg w \gg \lambda$. Typical dimensions: diameter = 21 mm; $w = 3$ mm.

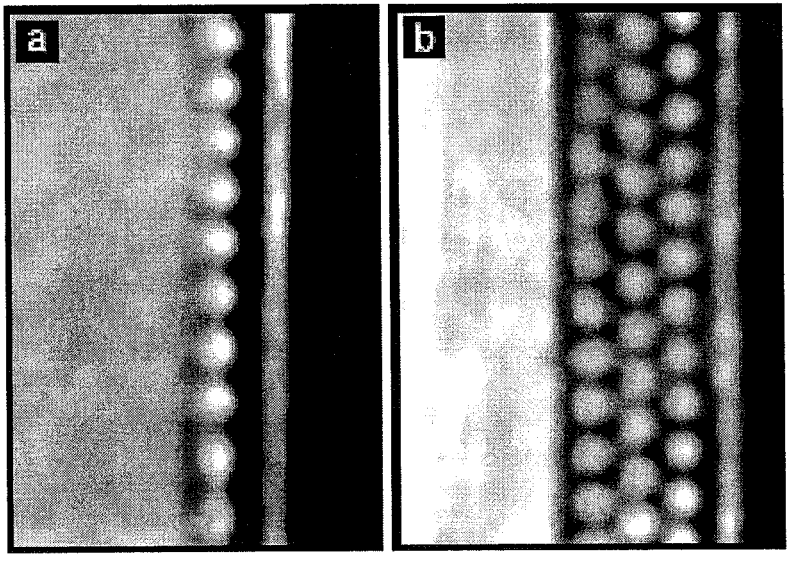

Fig. 2. Stationary concentration patterns in the thin strip gel reactor. Color contrast enhanced images corresponding to a central part of the reactor; view size 2.1 mm × 2.1 mm. Color code: dark, reduced iodine state; clear, oxidized iodine state. (a) Single row of clear spots parallel to the feed boundaries. (b) Multiple staggered rows of spots parallel to the feed boundaries.

when using the "gel strip reactor" (Fig. 1b), the reactor geometry that enabled the first experimental observation of Turing patterns.[4] When the CIMA reaction is operated in this reactor geometry, patterns commonly appear as one to four rows of clear spots set parallel to the feed boundaries and at a distance from these boundaries (Fig. 2). Besides the groundbreaking analytical results he obtained for the bifurcation to Turing patterns, G. Nicolis was also the first to consider the existence of ramps of parameters[2, 20] along one direction and their effects on the appearence of the structures. Analytical and numerical evaluations of the characteristics of the structure have been proposed[21, 22] but these works doa not take into consideration the cross coupling of spatial modes across the strip.[23, 24]

When a disc shaped reactor (Fig. 1c) is used, observations are made across the feed surfaces and, in this case, patterns are seen to spread over the whole view plane.[12, 25, 26] If the pattern stratum between the two feed surfaces is sufficiently confined ($\Delta \leqslant \lambda$), it is said that pattern develops in a monolayer.[27] The theoretically predicted[28, 29] standard two-dimensional hexagonal (Fig. 3a) and parallel stripe (Fig. 3b) planforms are observed. Different patterns correspond to different feed compositions.

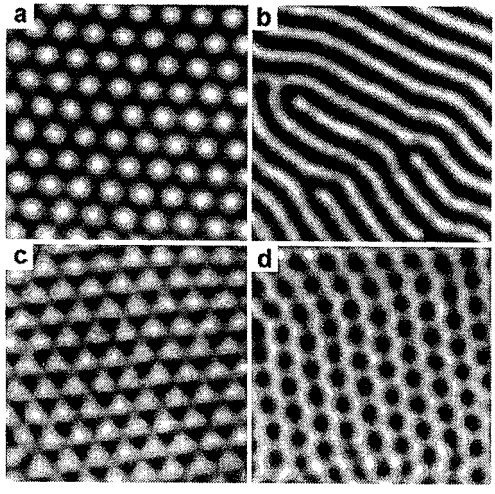

Fig. 3. Stationary planforms observed in the two-side-fed disc reactor operated with the CIMA reaction. Standard patterns: (a) hexagonal array of "clear" spots (b) array of parallel stripes (bands). Nonstandard patterns: (c) array of symmetric triangles (d) array of "dark" hexabands. All patterns are at the same scale: view size 1.7 mm × 1.7 mm.

If the pattern stratum is less confined ($\Delta > \lambda$), nonstandard two-dimensional patterns—triangles (Fig. 3c) or mixed planform patterns (Fig. 3d)—are viewed in the disc reactor.[26, 30, 31] The actual status of such unusual reaction–diffusion pattern planforms is still a matter of debate. Even if it is clear that the third dimension can play an essential role in the development of these patterns, it is unclear if they are the result of mere moiré effects due to the superposition of layers of standard hexagon and stripe planforms[26, 30] or if these unusual planform symmetries correspond to genuine new solutions of quasi-2D systems. A particular example is that of the so-called "black eye" hexagonal patterns that could be explained either from the activation of the overtones of the hexagonal modes[32] or as the projection of a bcc pattern, predicted by the standard 3D theory, correctly oriented by anisotropic effect of the feeding ramps.[33]

The three-dimensional characteristics of patterns are difficult to solve experimentally. Different indirect approaches have been attempted: In one of these, Ouyang *et al.*[11] show that in a two-side-fed reactor, the strong gradients of parameters seem to favour the stacking of two-dimensional patterns rather than the genuine three-dimensional structures predicted by the theory and which may be rather intricate as was discussed recently.

In another approach, experimenting in bevelled disc reactors (feed faces making an angle) confirms the above result and can even show a

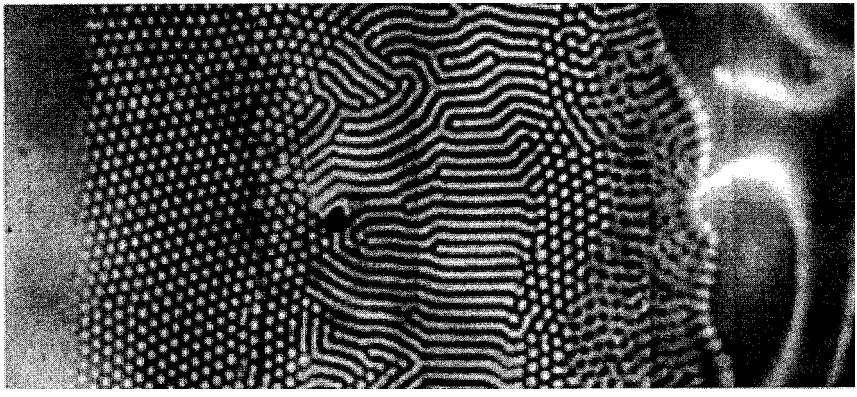

Fig. 4. Sequence of patterns in the bevelled disc. From left to right: uniform state, hexagonal array of spots, stripes, new hexagonal array of spots, superposition of dark spots and stripes, travelling waves. The circular faces of the bevelled disc (diameter 21 mm) make an angle of 4°; thickness of the disc: from 1.7 mm on the left to 3.2 mm on the right.

bifurcation from standing Turing patterns to wave patterns as a function of the disc thickness, as illustrated in Fig. 4.

Interestingly, the distance between the feed surfaces not only acts on the thickness of the pattern stratum so that one or more layers of patterns can develop but also, it can act as a genuine bifurcation parameter[30, 31, 34] as illustrated in Fig. 4. There, the thickness (w) of the disc increases continuously from left to right and one witnesses a sequence of patterns as the bifurcation diagram is unfolded in space. First, one can see a transition from the uniform state to an hexagonal array of clear spots then another to stripes. This corresponds to the standard pattern sequence predicted by theory for two-dimensional systems. Beyond the domain of stripes, a new domain of clear hexagons is followed by a domain of disordered dark hexagons before a region of wave patterns is reached on the right. These dark, reentrant hexagons are also well accounted by theoretical approaches for given parametric conditions. On the other hand, the waves appear because of the underlying Hopf bifurcation that has been shifted by the complexation effects and that leads to oscillatory behavior.

In two-side-fed reactors, the dimensionality of patterns cannot be directly controlled; it is a response of the system to chemical concentrations imposed at the feed surfaces. This can make observations difficult to interpret, as mentioned above. Furthermore, the large changes in chemical concentrations and in stoichiometric ratio of species between the two feed surfaces make quantitative modelling difficult since most of the tractable kinetical models are usually valid in restrained ranges of concentrations.

This introduces difficulties both for modeling and in experimental control of pattern dimensionality.

3. ONE-SIDE-FED REACTORS

To try to avoid some of the above difficulties, experiments are now more currently performed in thin one-side-fed reactors. In such reactors, all chemicals are introduced in a single reservoir (say reservoir 1 in Fig. 1a, while reservoir 2 is replaced by an impermeable wall). If the disc of gel is thin enough (typically (w) is made less than the pattern wavelength λ), one might expect that no significant concentration gradient develops in the thickness of the gel. Consequently, these reactors can be thought as good approximations of extended two-dimensional systems irrespective of chemical feed concentrations.

The dynamics of such a device is then described by the following set of equations which respectively describe reservoir 1 and the gel. In the first equation, one recognizes the local reaction kinetics term, the input-output term and the interaction term with the gel part of the device that involves the flux of matter through the boundary separating the two media. The second equation describes the reaction–diffusion processes that take place in the gel.

$$\frac{\partial c_i}{\partial t} = f(\mathbf{c}) + \frac{c_i - c_{i0}}{\tau} + \frac{\rho_V D_i}{w}\left(\frac{\partial c_i}{\partial r}\right)_{r=0} \tag{1}$$

$$\frac{\partial c_i}{\partial t} = f(\mathbf{c}) + D_i \nabla_r^2 c_i \tag{2}$$

where $\mathbf{c} = (..., c_i, ...)$ is the vector of the concentrations c_i, c_{i0} is the concentration of species i in the input flow, D_i its diffusion coefficient, τ is the residence time, ρ_V is the ratio of the volume of the gel to the volume of the CSTR, and w is the gel thickness.

On contact with reservoir 1, one imposes fixed concentration boundary conditions (equal to concentrations in reservoir 1), whereas no-flux conditions are taken along the other impermeable boundaries of the gel. If the ratio of the volume of the gel is small with respect to that of reservoir 1, the latter, since all chemicals are already present, then acts as a true continuous stirred thank reservoir (CSTR). A priori, this CSTR can exhibit any behavior of homogeneous nonlinear dynamical systems such as multistability, oscillations or even chaotic behavior. Until now, we have avoided the regions of parameters where the CSTR becomes self-oscillatory (or chaotic for that matter). In such regions, we would be dealing with the

more intricate situation of periodically forced spatio-temporal systems. Such type of reactor is also interesting as it allows direct correlations to be made between the dynamics in the CSTR and that in the gel.

Let us recall the characteristics of the CSTR. If the input flow is large—that is if the residence time is much shorter than the typical reaction time—the extent of the reaction is small and, in the stationary regime, the concentrations are close to the compositions in the flows (flow state F). If the residence time is much longer than the reaction time, the extent of the reaction is large and the composition in the reactor is near that of the thermodynamic equilibrium that one would obtain in a closed reactor with the same initial composition (thermodynamic state T). In standard reactions, the branches of states F and T are smoothly connected at intermediate flow rates, but when autocatalytic or similar nonlinear kinetic processes (as in the reactions we are studying) are present, the two states can exist for a same set of flow rates: their stability domains overlap (hence the bistability) over a range of control parameters, clearly defining two distinct branches F and T and the transition from one state to the other occurs with hysteresis. The transition from the monostable to the bistable situation often proceeds through conditions reminding a critical point where the transition from F to T, although smooth, is very sharp. Because of such properties, in one-side-fed reactors, it is convenient to distinguish systems for which the solution in the CSTR is in a monostable stationary state from those where it exhibits a bistability between two stationary states.

3.1. Monostable CSTR

When the feed solution in the CSTR exhibits a stationary monostable state, as it is the case with the CDIMA reaction, the classical two-dimensional hexagon and stripe patterns are observed[35] as we had already obtained in the two-side-fed reactor when a monolayer formed. Here however, the dimensionality is much better controlled. Accurate modeling, using the five variable kinetic model of the reaction proposed by Lengyel, Rabài, and Epstein,[16] for this system becomes possible. As illustrated in ref. 35, striking agreement between computational and experimental results may be obtained. In the phase diagram of Fig. 5, one can distinguish from left to right three types of regions: (i) a region of uniform stationary state, (ii) a region of stationary Turing patterns, (iii) a region of oscillations in the CSTR for which the corresponding dynamics in the gel is not considered.

In chemical systems, the penetration depth of the influence of boundary conditions and the pattern wavelength rely on the same competition

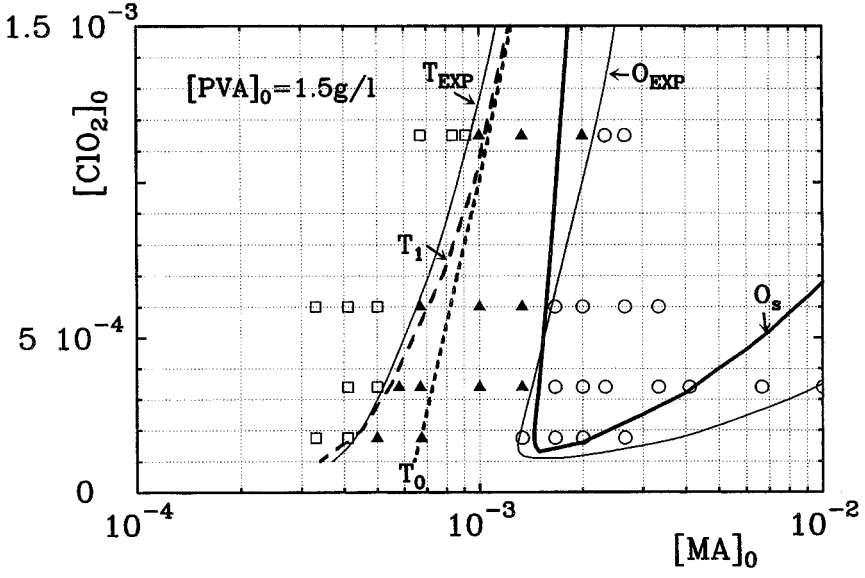

Fig. 5. Plane section ($[MA]_0$,$[ClO_2]_0$) of the pattern phase diagram. Experimental observations: white square, stationary uniform states; black triangle, Turing patterns; white circle, oscillatory states; thin full line, limit of Turing (T_{EXP}) and oscillatory (O_{EXP}) domains (estimated from these data). Numerical simulations: thick short dashed lines, Turing bifurcation (T_0); thick long dashed lines, limit of bistability between uniform and patterned states (T_1); thick full line, limit of oscillatory domain (O_S).

between reaction and diffusion and thus, should develop over comparable lengths. The homogeneity onto the feed face should then force uniformity across these thin gels, in planes parallel to this face. Surprisingly, patterns develop. This development relies, here, on the presence of a thin membrane that was, for technical reasons, inserted between the CSTR and the gel. It was shown theoretically and confirmed experimentally[35] that this additional interface introduces mixed boundary conditions which have different consequences for two types of species. Whereas this effect on the concentration of the input species (which are in large excess) remains small, these conditions are close to no-flux conditions for the intermediate species directly involved in the formation of Turing structures. Thus, the patterns are let free to develop in the direction parallel to the faces.

Such reactors naturally allows to follow the pattern growth dynamics. For some conditions, in the monostable region of the CSTR but close to the critical point for bistability, there exists a large difference in the levels of concentrations corresponding respectively to the F and T branches of the CSTR. The Turing patterns tend to form in the gel for parameters of

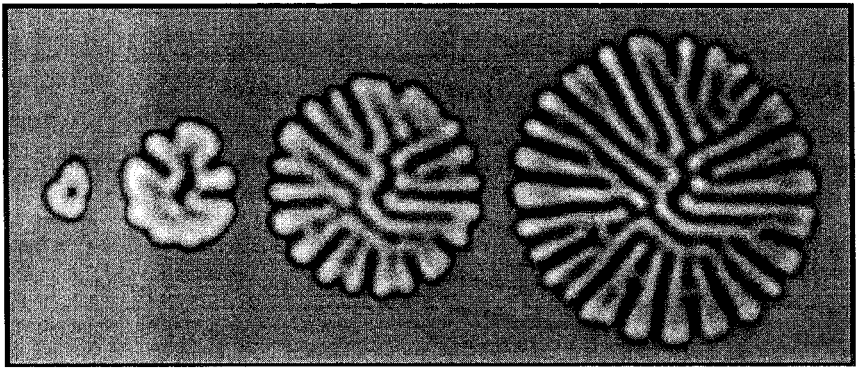

Fig. 6. Flower-like pattern. Pictures taken (a) 12 min; (b) 20 min; (c) 35 min; (d) 52 min after the initial growth of the pattern.

the CSTR corresponding to the vicinity of this critical point.[36] Furthermore, patterns develop behind a front that propagates into the previously existing uniform state that has now become unstable. What is remarkable is that this front exhibits morphological instabilities giving rise to growth modes involving spot division or finger splitting.[36] Figure 6 illustrates the finger tip splitting growth mechanism for Turing pattern which ultimately leads to stripes.

3.2. Bistable CSTR

When the CSTR evolves in its bistable region, as it can be the case for the CDI[37] (or also FIS[38]) reaction, a first important aspect is the determination of the possible corresponding states in the gel. Let one consider the situation along the direction orthogonal to the CSTR-gel reactor boundary, i.e., along the depth of the gel. If the CSTR is in the F branch, at each point along the gel, fresh reactants are brought by diffusion from the feeding edge, where the concentration is kept fixed. Close to this edge, the extent of the reaction is small and the chemical composition remains close to that of the flow branch. As we move away from this edge, the extent of the reaction becomes larger because the amount of fresh reactants that reaches the corresponding space point is limited by its transport through molecular diffusion. So, if the gel film is thick enough, the regions of the gel far from the feeding edge may eventually belong to a state laying on the T branch. In such a case, the composition changes from branch F to branch T somewhere inside the gel. Thus, for the same F state in the CSTR, one may observe two quite different composition profiles as a function of w, the thickness of the gel. If w is very small, the chemical composition in the gel

stays near or in the direct continuity of the F state of the CSTR. By extension, we also call F this state in the gel. If w is large enough, the part of the gel close to the CSTR remains on branch F while the opposing part has the T composition. We call FT this mixed state of the gel. It can be shown theoretically and experimentally that the stability of the F and FT states of the gel can overlap for some finite range of w.[37, 39] Thus, two concentration profiles that fit the same homogeneous conditions at the CSTR/gel boundary can be observed in the gel. This is illustrated in Fig. 7, obtained in a thin annular strip of gel fed along one edge. This multiplicity phenomenon has been dubbed "spatial bistability." When the experiments

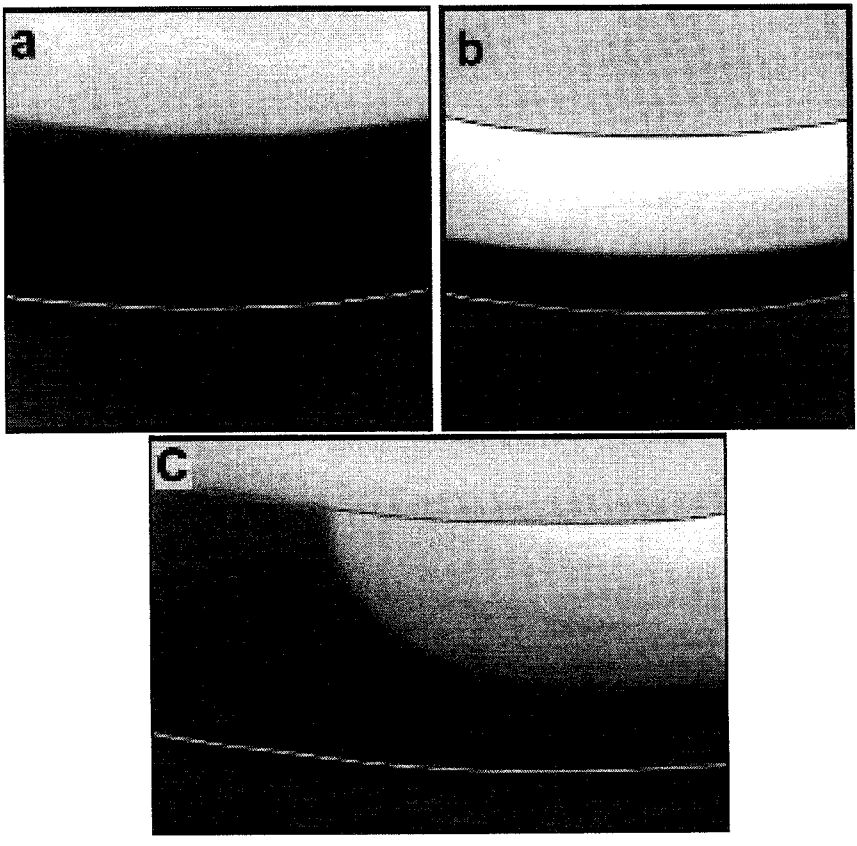

Fig. 7. Spatial bistability in the one-side-fed annular reactor. (a) state F; (b) state FT; (c) interface between the F and FT states. The arc-lines are the limits of the gel. The lower arc delineates the CSTR interface, the upper arc delineates the impermeable wall. Distance between the two arc-lines, w = 1 mm.

are made in a disc reactor, the detection of the pattern is made by integration of the light over the thickness of the gel. The two states are still revealed by different color densities. Different domains corresponding to states F and FT can coexist in the film. At the interface between F and FT, the connecting front exhibits a strong curvature in order to join up orthogonally with the impermeable wall. Such a connecting front is shown Fig. 7c in an annular strip reactor. The relative stability of the two states (F and FT) may be apprehended by studying the dynamics of this F–FT interface. Patterns may form when various such interfaces are present and are stabilized by nonvariational effects. This would provide a comprehensive understanding of the pattern observed in a disc reactor when operating the FIS reaction.[38] The possibility that periodic structures develop on the basis of a similar spatial bistability has been recently shown theoretically.[40] However, it should be clear from the preceding discussion that such patterns are not genuine 2D patterns and do not behave as predicted by the classical two-dimensional model approximation.

4. CONCLUSION

Many successes have been gathered in the explanation of the experimental results by dissecting the problem in various dimensions. Nevertheless a complete and unified interpretation will have to resort to the consideration of the full 3D aspects. Because of the high number of variables appearing in the kinetic mechanism, theoretical analysis is difficult, even if one forgets the inhomogeneity of conditions imposed by the reactors. This paper has also emphasized the role of the experimental apparatus which completely defines the nature of the boundary conditions, a point that is often ignored in the literature. It is often flimsily assumed that the thinnest is the system, the closest it is to a genuine two-dimensional system. This is obviously wrong since the role of the specific boundary conditions increases when the gel thickness decreases. Actually, we have shown that this thickness can even become a bifurcation parameter and control the formation of patterns. We believe that a number of observations in these reactors should be revisited in regard to these considerations.

ACKNOWLEDGMENTS

The review includes work obtained in collaboration with M. Bachir, E. Barillot, P. Blanchedeau, V. Dufiet, S. Métens, and B. Rudovics. AD, GD, PB thank the F.N.R.S. (Belgium and the Van Buuren Foundation for their support. This research was sponsored through a C.G.R.I.-F.N.R.S./C.N.R.S. grant.

REFERENCES

1. A. M. Turing, *Philos. Trans. R. S. London*, *B* **327**:37 (1952).
2. J. F. G. Auchmuty and G. Nicolis, *Bull. Math. Biol.* **37**:323 (1975).
3. G. Nicolis and I. Prigogine, *Self Organization in Nonequilibrium Systems* (Wiley, New York, 1977).
4. V. Castets, E. Dulos, J. Boissonade, and P. De Kepper, *Phys. Rev. Lett.* **64**:2953 (1990).
5. D. Walgraef, G. Dewel, and P. Borckmans, *Adv. Chem. Phys.* **49**:311 (1982); A. De Wit, P Borckmans, G. Dewel, and D. Walgraef, *Physica D* **61**:289 (1992).
6. P. Borckmans, G. Dewel, A. De Wit, and D. Walgraef, in *Chemical Waves and Patterns*, Chap. 10, Understanding Chemical Reactivity, Vol. 10, R. Kapral and K. Showalter, eds. (Kluwer Academic Publisher, 1994).
7. A. De Wit, *Adv. Chem. Phys.* **109**:435 (1999).
8. A. De Wit, P. Borckmans, and G. Dewel, *Proc. Nat. Acad. Sci. (USA)* **94**:12765 (1997).
9. T. Ohta, M. Mimura, and P. Kobayashi, *Physica D* **34**:115 (1989).
10. A. Hagberg and E. Meron, *Phys. Rev. E* **48**:705 (1993); A. Hagberg and E. Meron, *Non Linearity* **7**:805 (1994); A. Hagberg and E. Meron, *Chaos* **4**:477 (1994); A. Hagberg, E. Meron, I. Rubinstein, and B. Zaltman, *Phys. Rev. E* **55**:4450 (1997).
11. Q. Ouyang, Z. Noszticzius, and H. L. Swinney, *J. Chem. Phys.* **96**:6773 (1992).
12. P. De Kepper, J. J. Perraud, B. Rudovics, and E. Dulos, *Int. J. Bif. Chaos* **4**:1215 (1994); J. J. Perraud, A. De Wit, E. Dulos, P. De Kepper, G. Dewel, and P. Borckmans, *Phys. Rev. Lett.* **71**:1272 (1993).
13. H. Kidachi, *Prog. Theor. Phys.* **63**:1152 (1980).
14. A. Rovinsky and M. Menzinger, *Phys. Rev. A* **46**:6315 (1992).
15. A. De Wit, D. Lima, G. Dewel, and P. Borckmans, *Phys. Rev. E* **54**:261 (1996).
16. I. Lengyel, G. Rabai, and I. R. Epstein, *J. Am. Chem. Soc.* **112**:4606 (1990); I. Lengyel, G. Rabai, and I. R. Epstein, *J. Am. Chem. Soc.* **112**:9104 (1990); I. Lengyel, J. Li, K. Kustin, and I. R. Epstein, *J. Am. Chem. Soc.* **118**:3708 (1996).
17. I. Lengyel and I. R. Epstein, *Science* **251**:650 (1990); I. Lengyel and I. R. Epstein, *Proc. Nat. Sci. (USA)* **89**:3977 (1992).
18. J. E. Pearson and W. J. Bruno, *Chaos* **2**:513 (1992).
19. J. Boissonade, *J. Phys. France* **49**:541–546 (1988).
20. M. Herschkowitz-Kaufman and G. Nicolis, *J. Chem. Phys.* **56**:1890 (1972).
21. S. Kadar, I. Lengeyl, and I. R. Epstein, *J. Phys. Chem.* **99**:4054 (1995).
22. S. Setayeshgar and M. C. Cross, *Phys. Rev. E* **58**:4485 (1998).
23. V. Dufiet and J. Boissonade, *Phys. Rev. E* **53**:4883 (1996).
24. P. Borckmans, A. De Wit, and G. Dewel, *Physica A* **188**:137 (1992).
25. Q. Ouyang and H. L. Swinney, *Nature* **352**:610 (1991).
26. B. Rudovics, E. Dulos, and P. De Kepper, *Physica Scripta T* **67**:43 (1996).
27. V. Dufiet and J. Boissonade, *Physica A* **188**:158 (1992).
28. G. Dewel, P. Borckmans, and D. Walgraef, *J. Phys. C* **12**:L491 (1979); D. Walgraef, G. Dewel, and P. Borckmans, *Phys. Rev. A* **21**:397 (1980); D. Walgraef, G. Dewel, and P. Borckmans, *Adv. Chem. Phys.* **49**:311 (1982).
29. L. M. Pismen, *J. Chem. Phys.* **72**:1900 (1980).
30. E. Dulos, P. Davies, B. Rudovics, and P. De Kepper, *Physica D* **98**:53 (1996).
31. B. Rudovics, Ph.D. Thesis (Bordeaux, 1995).
32. Q. Ouyang, G. H. Gunaratne, and H. L. Swinney, *Chaos* **3**:707 (1993).
33. M. G. M. Gomes, *Phys. Rev. E* **60**:3741 (1999).

34. E. Dulos, A. Hunding, J. Boissonade, and P. De Kepper, in *Transport and Structure: Their Competitive Roles in Biophysics and Chemistry*, Lecture Notes in Physics, Vol. 352, S. C. Mueller, J. Paosi, and W. Zimmermann, eds., to appear.
35. B. Rudovics, E. Barillot, P. W. Davies, E. Dulos, J. Boissonade, and P. De Kepper, *J. Phys. Chem.* **103**:1790 (1999).
36. P. W. Davies, P. Blanchedeau, E. Dulos, and P. De Kepper, *J. Chem. Phys.* **102**:8236 (1998).
37. P. Blanchedeau, J. Boissonade, and P. De Kepper, *Physica D*, submitted.
38. K. J. Lee, D. McCormick, Q. Ouyang, and H. L. Swinney, *Science* **261**:192 (1993); K. J. Lee and H. L. Swinney, *Phys. Rev. E* **51**:1899 (1995).
39. P. Blanchedeau and J. Boissonade, *Phys. Rev. Lett.* **81**:5007 (1998).
40. M. Bachir, P. Borckmans, and G. Dewel, *Phys. Rev. E* **59**:86223 (1999).